Letter to the Editor

Intramedullary spinal cord metastases and whole body ^{18}F-FDG PET-CT—A case report

Geetika Bhatt[1], Angita Jain[2], Aashish Bhatt[3], Ali Cahid Civelek[4]

[1]Department of Hematology/Oncology, University Hospitals, Case Western Reserve University, Cleveland, OH, USA; [2]The Atwal Clinic, Jacksonville, FL, USA; [3]Department of Radiation Oncology, University Hospitals, Case Western Reserve University, Cleveland, OH, USA; [4]Johns Hopkins Medical Institutions, Division of Nuclear Medicine and Molecular Imaging, Baltimore, MD, USA

Correspondence to: Ali Cahid Civelek, MD. Johns Hopkins Medical Institutions, Division of Nuclear Medicine and Molecular Imaging, 601 N Caroline St, JHOC 3225, Baltimore, MD 21287, USA. Email: acivele1@jhmi.edu.

Submitted Feb 07, 2019. Accepted for publication Mar 01, 2019.
doi: 10.21037/qims.2019.03.05
View this article at: http://dx.doi.org/10.21037/qims.2019.03.05

Introduction

Intramedullary spinal cord metastases (ISCM) are neurological complications of cancer which can be devastating to quality of life of a patient. Early diagnosis and initiation of appropriate treatment can prevent paralysis, bowel and bladder incontinence and prevent drastic changes to the quality of life of a cancer patient. However, signs and symptoms occur late in disease and diagnosis before signs may remain a challenge. With the widespread use of positron emission tomography-computed tomography (PET-CT) scans for cancer staging, one should be cognizant to not overlook the presence of hypermetabolic FDG avid metastatic lesion along the spinal cord, especially when there is multiple FDG avid metastatic disease present.

Case presentation

A 55-year-old female with a 40 pack year history of smoking and no other past medical history presented to her primary care physician with 2 weeks of low-grade fever, chest congestion, and right-sided pleuritic chest pain, and a 20-pound weight loss over the last six months. Chest X-ray showed a right lung mass. CT scan of the chest revealed a 3.9 cm × 6.2 cm right hilar mass encasing the right main bronchus, extending medially to the carina and abutting the superior vena cava and right pulmonary artery, and mediastinal lymphadenopathy. Her pulmonologist performed a bronchoscopy assisted biopsy of the right hilar mass and sampled mediastinal lymph nodes, which revealed stage T3N2 small cell carcinoma of the lung with the involvement of the ipsilateral mediastinal lymph nodes. Her MRI brain ordered by her medical oncologist revealed multiple intracranial lesions including left cerebellum and the frontal lobe. She subsequently received treatment with six cycles of cisplatin and etoposide as per National Comprehensive Cancer Network (NCCN) guidelines and whole brain irradiation. She had partial remission and remained on surveillance for 6 months, after which her disease started to progress with an increase in the size of her right lung mass, mediastinal adenopathy and multiple new osseous lesions involving the lumbar spine. She received systemic therapy for her relapsed disease with topotecan as it had been around 6 months since her last treatment. Treatment with topotecan discontinued after only 2 months due to significant diarrhea and resulted in a hospitalization. Docetaxel treatment started and her disease stabilized. She also received chest irradiation of the right lung mass and mediastinal lymph nodes. In 20 months, she had three lines of systemic chemotherapy as well as whole brain and chest irradiation for her multiple recurrences. At about 24 months after initiation of her therapy, she developed a painful left hip and left femur bone metastases.

She was then referred to our center at the University of Louisville Hospital for management of her recurrent disease. Physical examination revealed tenderness in the left hip without any weakness in her legs, pain in her spine, and bowel or bladder incontinence at that time. A re-staging whole body PET-CT scan revealed FDG avid

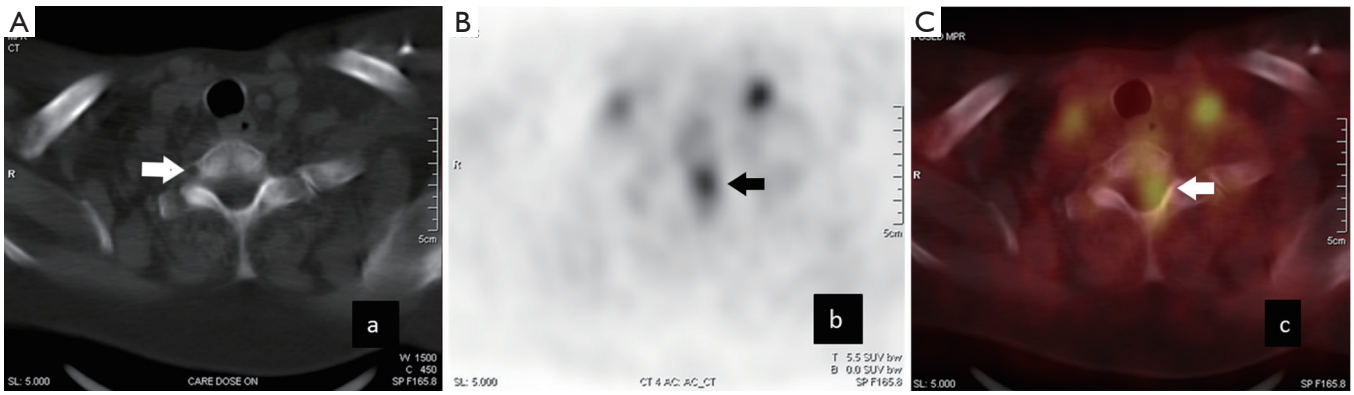

Figure 1 Transaxial images of the hypermetabolic lesion in the spinal cord. Transaxial non-contrast CT of the chest displayed in the bone window (A) shows no bone abnormality (white arrow). Same level transaxial 18F-FDG PET (B) and PET-CT fused image (C) show abnormal hypermetabolic uptake in the spinal cord (black and white arrows respectively) at the level of T1 with a standardized uptake value (SUV) max of 4.2. (Liver SUV average: 2.7, SUVmax: 3.0). There are two anterior mediastinal lesions present as well.

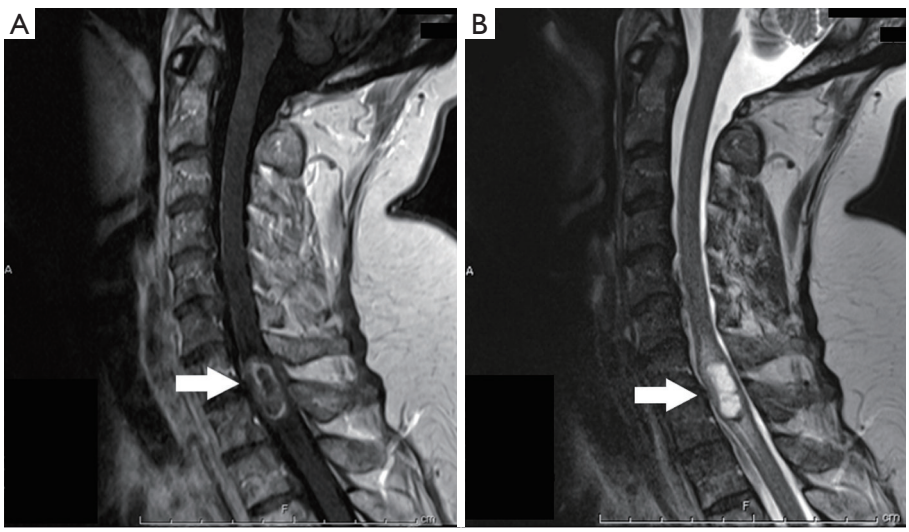

Figure 2 Magnetic resonance image (MRI) of the cervical spine. A sagittal contrast-enhanced T1 weighted (A) and T2 weighted (B) MRI of the cervical spine shows 2 cm peripherally enhancing intramedullary lesion with a central cystic component, extending craniocaudally from the level of C7 to T1 (white arrows).

hypermetabolic mediastinal lymphadenopathy, multiple bony lesions in the lumbar spine, left proximal femur and left sacroiliac joint. There was also a focus of intense FDG avid lesion in the spinal cord at the T1 level, raising the probability of an intramedullary spinal cord metastasis (*Figure 1*). MRI scan of her spine showed a 2 cm enhancing intramedullary lesion extending craniocaudally from the level of C7 to T1 with a central cystic component, consistent with a drop metastasis (*Figure 2*). The patient received a palliative radiation treatment with 20 Gray in 5 fractions for pain control and stabilization of bone (*Figure 3*). Systemic therapy with Vinorelbine initiated, but the patient developed worsening mental status with new brain lesions and ultimately, succumbed to her disease, without experiencing complications specific to her C7-T1 spinal cord metastasis.

Discussion

Central nervous system (CNS) metastases to the

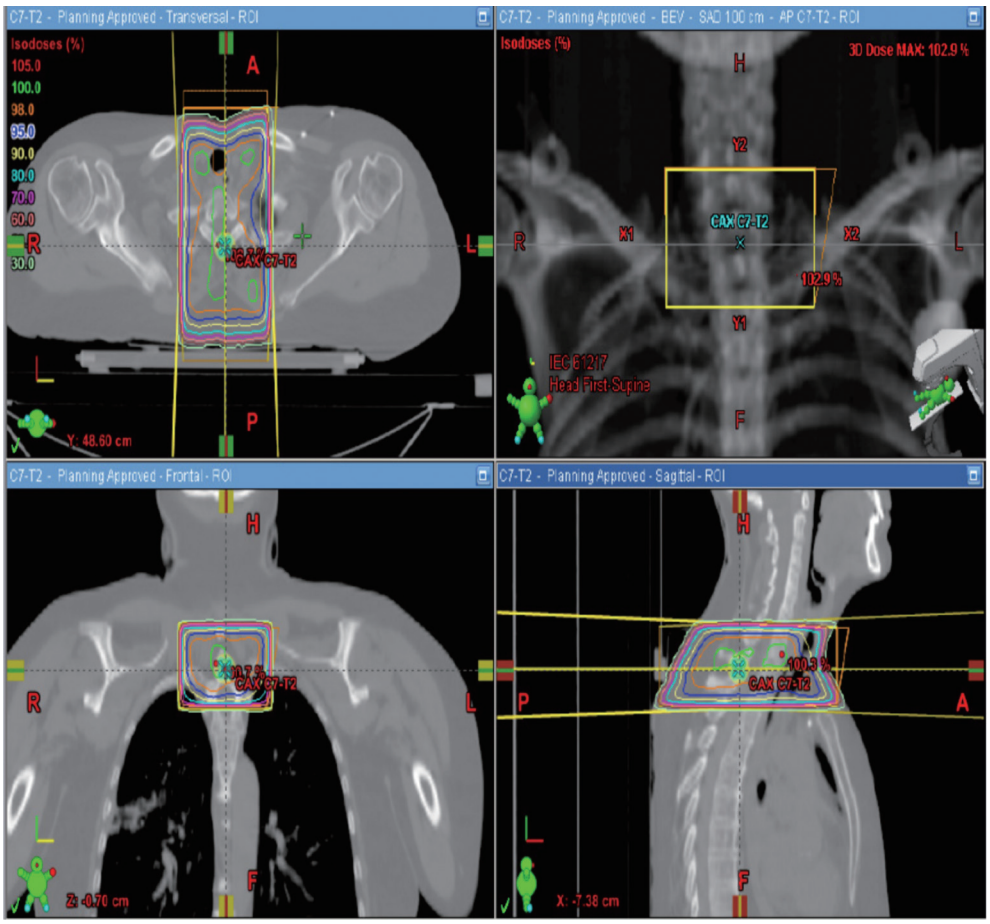

Figure 3 Radiation treatment fields. T1 lesion treated with anterior-posterior and posterior-anterior fields encompassing C7-T2 spine. Isodose lines in axial, coronal and sagittal sections, show the dose distribution delivering a total dose of 20 Gray in 5 fractions.

intramedullary spinal cord are rare constituting only about 8–9% of all CNS metastases (1,2). They can arise anytime between 2 months to up to 15 years after the initial diagnosis (1). Most originates from lung cancer (50%), with the remaining from breast cancer (11%), colorectal cancer (3%), kidney cancer (10%), melanomas (8%) and lymphomas (4%) (1,3). ISCM is associated with synchronous brain metastases (33%) and meningeal carcinomatosis (25%) (4).

In contrast to primary intramedullary tumors, the hallmark symptoms of ISCM are the rapid progression of pain and lower extremity weakness within hours to days (1,5). Sensory loss and urinary incontinence occur later in the course of the disease. In contrast to epidural lesions, pain is more ubiquitous and less severe (*Figure 4*). Brown-Sequard syndrome or a strong asymmetry in myelopathy noted in almost half of the patients with ISCM (30–45%) but only 3% of epidural metastases (5,6). Though ISCM may occur at every level of the spinal cord, the cervical spinal cord is the most common site, which may be related to its higher bulk and rich vascular supply (1).

The diagnosis can be established with gadolinium-enhanced MRI or with the use of 2-deoxy-2-(^{18}F) fluoro-D-glucose (^{18}F-FDG) PET-CT as demonstrated in this case report. Although whole body ^{18}F-FDG PET-CT is usually not well suited for the detection of brain metastases owing to the high baseline FDG activity present in the normal gray matter cortical brain tissue. On the other hand, the spinal cord is structurally mostly white brain matter, thus, has much lower FGD metabolic activity. When a spinal cord metastasis is present, this feature provided a more favorable tumor-to-background FDG contrast and making metastatic lesions more amenable for detection on whole body PET-CT scans (7,8). Whole body ^{18}F -FDG PET was

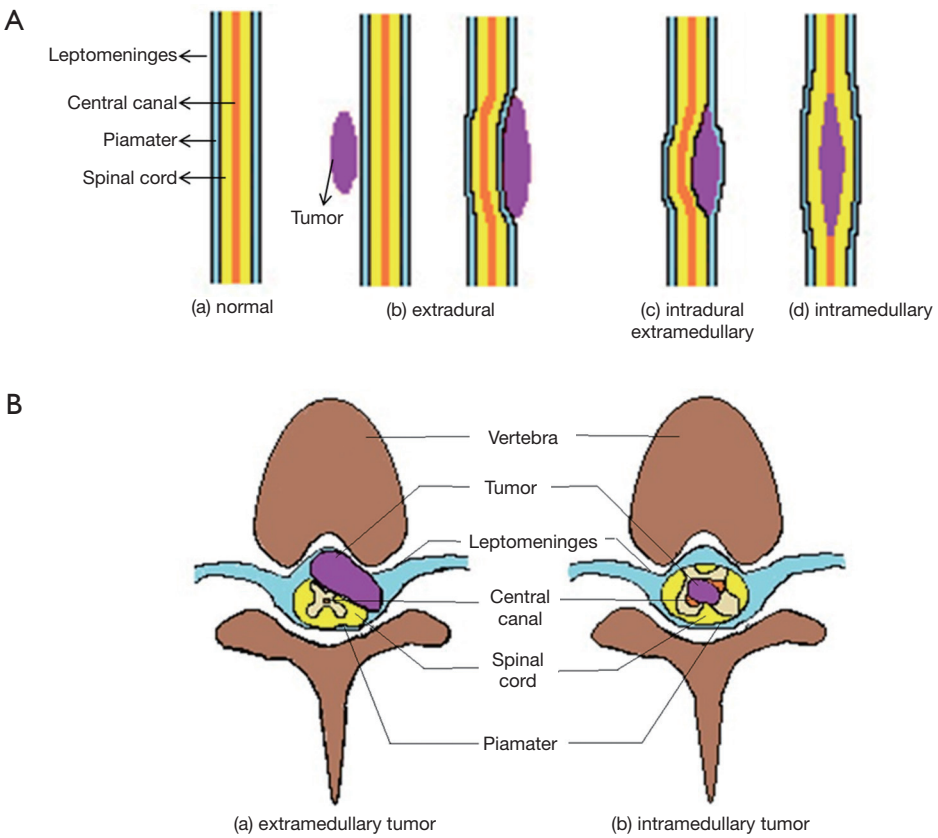

Figure 4 Schematic demonstration of the spinal cord metastatic lesions and illustrating their locations: extradural (b), intradural-extramedullary (c), and intramedullary (d) tumors in coronal (A) and axial (B) sections. (a) Depicts the appearance of a normal spinal cord.

noted to have 96% sensitivity and 50% specificity for spinal cord metastases in patients with cancer, and 97% sensitivity for non-sclerotic lesions and 95% sensitivity for sclerotic bone lesions when confirmed with a biopsy (9). Recent studies with whole-body MRI utilizing parallel imaging techniques to combine MRI and PET-CT data, have shown increased specificity of PET (100%) compared to MRI (80%), equal diagnostic accuracy, but a decreased sensitivity (91% compared to 100%) in detection of distant metastases in patient to patient analysis (10). Despite such enhanced diagnostic capability, ^{18}F-FDG PET images may not be able to accurately differentiate an intramedullary spinal cord metastasis from an epidural tumor due to lack of sufficient image resolution. A gadolinium-enhanced MRI is needed to establish such localization and confirmation.

Once the diagnosis is confirmed, treatment with steroids, and radiation or chemotherapy, or a combination of all, should be initiated promptly, as was done in our patient. Patients with ISCM have a poor prognosis with a mortality rate of 80% within 3–4 months, which may be related to the presence of widespread metastatic disease in these patients. Early initiation of the treatment can stabilize or reverse neurological deficits, thus preserving ambulation and quality of the remaining life of the patient, which what happened in the case presented.

A word of caution is that there is physiological relative increased elongated area of ^{18}F-FDG uptake consistently visualized in the cervical spinal cord peaking at C4 level, and in the lower thoracic spinal cord peaking at the T11-T12 segments, with intensities nearly as high as 30% greater than the liver FDG intensity, both with visual or semi-quantitative assessment (SUV value). Although various theories proposed, the cause of this physiologic FDG uptake is indeterminate (11); the interpreting physicians should be aware of this pitfall.

Conclusions

Detection of ISCM can help in early initiation of treatment to reverse neurological deficits and improve the quality

of the remaining life of cancer patients. Whole-body ^{18}F-FDG PET-CT can serve as an essential adjunct to MRI in identifying FDG avid metastatic spinal cord lesions and directing an enhanced MRI study for precise localization and confirmation of such tumors.

This case report points out the synergistic effect of Whole-body ^{18}F-FDG PET-CT scan to gadolinium-enhanced MRI. It does not imply the superiority of one test over the other and reminds interpreting physicians that they should be mindful to the compromised spinal cord, and look for the presence of possible spinal cord metastasis even while evaluating grossly abnormal whole body PET-CT scans with numerous metastatic lesions.

Acknowledgements

None.

Footnote

Conflicts of Interest: The authors have no conflicts of interest to declare.

Informed Consent: The study performed at the University of the Louisville Hospital, and the IRB waiver the need for the Informed Consent for this case report.

References

1. Kalayci M, Cagavi F, Gul S, Yenidunya S, Acikgoz B. Intramedullary spinal cord metastases: diagnosis and treatment - an illustrated review. Acta Neurochir (Wien) 2004;146:1347-54; discussion 1354.
2. Pellegrini D, Quezel MA, Bruetman JE. Intramedullary spinal cord metastasis. Arch Neurol 2009;66:1422.
3. Potti A, Abdel-Raheem M, Levitt R, Schell DA, Mehdi SA. Intramedullary spinal cord metastases (ISCM) and non-small cell lung carcinoma (NSCLC): clinical patterns, diagnosis and therapeutic considerations. Lung Cancer 2001;31:319-23.
4. Lee SS, Kim MK, Sym SJ, Kim SW, Kim WK, Kim SB, Ahn JH. Intramedullary spinal cord metastases: a single-institution experience. J Neurooncol 2007;84:85-9.
5. Sciubba DM, Petteys RJ, Dekutoski MB, Fisher CG, Fehlings MG, Ondra SL, Rhines LD, Gokaslan ZL. Diagnosis and management of metastatic spine disease. J Neurosurg Spine 2010;13:94-108.
6. Mut M, Schiff D, Shaffrey ME. Metastasis to nervous system: spinal epidural and intramedullary metastases. J Neurooncol 2005;75:43-56.
7. Sandu N, Popperl G, Toubert ME, Spiriev T, Arasho B, Orabi M, Schaller B. Current molecular imaging of spinal tumors in clinical practice. Mol Med 2011;17:308-16.
8. Di Chiro G, Oldfield E, Bairamian D, Patronas NJ, Brooks RA, Mansi L, Smith BH, Kornblith PL, Margolin R. Metabolic imaging of the brain stem and spinal cord: studies with positron emission tomography using 18F-2-deoxyglucose in normal and pathological cases. J Comput Assist Tomogr 1983;7:937-45.
9. Laufer I, Lis E, Pisinski L, Akhurst T, Bilsky MH. The accuracy of ((18)F)fluorodeoxyglucose positron emission tomography as confirmed by biopsy in the diagnosis of spine metastases in a cancer population. Neurosurgery 2009;64:107-13; discussion 113-04.
10. Schmidt GP, Schoenberg SO, Schmid R, Stahl R, Tiling R, Becker CR, Reiser MF, Baur-Melnyk A. Screening for bone metastases: whole-body MRI using a 32-channel system versus dual-modality PET-CT. Eur Radiol 2007;17:939-49.
11. Bhatt G, Li XF, Jain A, Sharma VR, Pan J, Rai A, Rai SN, Civelek AC. Study evaluating the normal variant 18F-FDG uptake in the lower thoracic spinal cord segments in cancer patients without CNS malignancy. Am J Nucl Med Mol Imaging 2013;3:317-25.

Cite this article as: Bhatt G, Jain A, Bhatt A, Civelek AC. Intramedullary spinal cord metastases and whole body ^{18}F-FDG PET-CT—A case report. Quant Imaging Med Surg 2019;9(3):530-534. doi: 10.21037/qims.2019.03.05

